Acta Geochim (2016) 35(4):428–436
DOI 10.1007/s11631-016-0107-5

ORIGINAL ARTICLE

Geochemistry of sedimentary rocks from Permian–Triassic boundary sections of Tethys Himalaya: implications for paleo-weathering, provenance, and tectonic setting

Akhtar R. Mir[1] · V. Balaram[2] · Javid A. Ganai[1] · Shamim A. Dar[3] · A. Keshav Krishna[2]

Received: 11 January 2016 / Revised: 6 February 2016 / Accepted: 18 April 2016 / Published online: 20 June 2016

Abstract The geochemical characteristics of two sections—the Permian–Triassic boundary (PTB) Guryul Ravine section, Kashmir Valley, Jammu and Kashmir, India; and the Attargoo section, Spiti Valley, Himachal Pradesh, India—have been studied in the context of provenance, paleo-weathering, and plate tectonic setting. These sections represent the siliciclastic sedimentary sequence from the Tethys Himalaya. The PTB siliciclastic sedimentary sequence in these regions primarily consists of sandstones and shales with variable thickness. Present studied sandstones and shales of both sections had chemical index of alteration values between 65 and 74; such values reveal low-to-moderate degree of chemical weathering. The chemical index of weathering in studied samples ranged from 71 to 94, suggesting a minor K-metasomatism effect on these samples. Plagioclase index of alteration in studied sections ranged from 68 to 92, indicating a moderate degree of weathering of plagioclase feldspars. The provenance discriminant function diagram suggests that the detritus involved in the formation of present studied siliciclastic sedimentary rocks fall in quartzose sedimentary and felsic igneous provenances. These sediments were deposited in a passive continental margin plate tectonic setting according to their location on a Si_2O versus K_2O/Na_2O tectonic setting diagram.

✉ Javid A. Ganai
jganai.ganai9@gmail.com

[1] Department of Earth Sciences, University of Kashmir, Srinagar 190006, India

[2] CSIR-National Geophysical Research Institute, Hyderabad 500007, India

[3] Department of Geology, S.P. College, Srinagar 190008, India

Keywords Geochemistry · Permian–Triassic boundary · Guryul Ravine · Tectonic settings

1 Introduction

The sedimentary succession of the Tethys Himalaya stretching from North India to South Tibet represents the deformed remnants of the northern continental margin of the Indian subcontinent. The succession, one of the most complete and spectacularly exposed in the world, preserves an excellent stratigraphic record of the history of Gondwana during most of the Phanerozoic. The global stratotype section and point (GSSP) for the Permian–Triassic boundary (PTB) (e.g. Meishan, Ursula Creek, Guryul Ravine, and Attargoo sections, etc.) have been a focus of researchers all over the world due to some important events like mass extinction, formation of the Neo-Tethys Sea, marine anoxia, increase of atmospheric CO_2 content, global warming, carbon isotopic excursion, acid rain, etc. (Wignall and Twitchett 1996; Berner 2002; Maruoka et al. 2003; Benton et al. 2004; Payne et al. 2004; Erwin 2005; Huey and Ward 2005; Brookfield et al. 2010; Shen and Lin 2010; Shen et al. 2011; Xu and Lin 2014). Various studies throughout the world have been carried out on clastic sedimentary rocks using major-, trace-, or rare earth element data to understand paleo-weathering, paleoclimate, provenance, tectonic setting, paleoredox conditions, and crustal evolution (Zhang et al. 2010; Sun et al. 2011; Wani and Mondle 2011; Ganai et al. 2014; Mir et al. 2015). Despite the global importance of PTB sections, little attention has been paid to geochemical characteristics of PTB sections of the northwest Himalaya (e.g. Guryul Ravine and Attargoo sections) (notable exceptions include Bhargava 2008; Williams et al. 2012; Ganai et al. 2014).

However, increasing attention has been paid to the paleontology and stratigraphy of the PTB Guryul section, with field-based work concentrated on assigning ages to the rock sequences and delineating depositional environments (Kapoor 1992, 1996; Yin et al. 2001; Brookfield et al. 2003, 2013). In the present study, we present geochemical data from the PTB sequences in the Kashmir and Spiti regions, North India, with an aim to understand the paleoweathering, provenance, and tectonic setting of these sections. This work adds to existing knowledge of the PTB Guryul Ravine and Attargoo sections and contributes to efforts to correlate geochemical characteristics among PTB sections of the world.

2 Geology of the study area

Rifting and eruption of middle Permian basalts was followed by separation of blocks of the northern edge of Gondwanaland, birth of the Neo-Tethys ocean, and rapid thermal subsidence of the northern Gondwana margin during Upper Permian and Triassic times. Due to this rapid subsidence, continuous sedimentation across the PTB took place on the northern Gondwanaland shelf (Myrow et al. 2003; Sciunnach and Garzanti 2012). The Permian–Triassic sedimentation sequence is well-preserved at Guryul Ravine (Kashmir Valley, India) and in the Permian Gungri Formation at Attargoo (Spiti Valley, India). These locations are considered to have the most complete and well-preserved PTB type-sections in the world.

The Kashmir Valley occupies an oval shaped basin between the Pir Panjal Range in the southwest and the Great Himalayan Range in the northeast. Permian–Triassic outcrops are exposed at various places in the Kashmir Valley e.g. Guryul Ravine, Phalgam, Ashmukam, etc. Guryul Ravine is considered GSSP for the PTB (Fig. 1a) (Kapoor 1996; Yin et al. 2001; Brookfield et al. 2003, 2010). The Guryul Ravine section consists of a conformable succession of mixed siliciclastic-carbonate sediments (>100 m thick) deposited in a deep-shelf or ramp setting (Brookfield et al. 2010). The Permo-Triassic sequences in Kashmir Valley are divided into the Zewan Formation of Upper Permian age and the overlying Lower Triassic Khunamuh Formation (Fig. 2a, b). The Panjal Traps, which are chiefly basaltic in composition with subsidiary association of silicic volcanic rocks, lie at the base of the Guryul Ravine section. The Zewan Formation is subdivided into four members named A, B, C, and D by Nakazawa et al. (1975).

The top-most 5 meters of the Zewan Formation are composed of fine- to medium-grained layers of sandy limestones or calcareous quartz sandstones interbedded with patchy calcareous shales (Brookfield et al. 2003). The transition from parallel lamination to hummocky cross-lamination structures suggests decreasing storm activity through time (Saito 1989; Brookfield et al. 2003). These cross-laminated and bioturbated well-sorted sands with a scarcity of fossils likely originated in a near-shore lagoon with graded storm beds transitioning shoreward to higher energy deposits (Brookfield et al. 2003, 2010). The Zewan Formation is overlain by the Khunamuh Formation, which is divided into six members, named as E, F, G, H, I, and J on the basis of variation in carbonate content (Nakazawa et al. 1975). Interbedded dark calcareous shales and argillaceous limestones (about 16 m thick) comprise basal parts of the Khunamuh Formation while upper members consist of shale, thin-bedded lime mudstone, and nodular limestone (Nakazawa et al 1975; Nakazawa and Kapoor 1981; Kapoor 1996; Brookfield et al. 2003).

Spiti is located in the northern part of the Himachal Pradesh, which occupies a central position in the Western Himalaya (Fig. 1b). The section exposed at Attargoo village (Fig. 2c, d) is composed of Permian gray-black shales of the Gungri Formation and Triassic limestones of the Mikim Formation. Since the Uppermost Permian strata have not been observed here, the cross-boundary biostratigraphy is yet to be confirmed (Garzanti et al. 1998; Williams et al. 2012). An upward progression from gray to black in the Gungri Shale supports the hypothesis that oxygen levels were decreasing toward the end of the Permian (Shukla et al. 2002). The Gungri Formation is mostly composed of black splintery shale and interbedded calcareous and micaceous siltstone (Singh et al. 1995). The silty shale mostly occurs in the base of the Gungri Formation, whereas the upper part contains gray-to-black shale capped unconformably by an iron-rich pebble-sand layer ("ferruginous layer") 2–8 cm in thickness marking, apparently, the PTB (Singh et al. 2004). Three factors point to the ferruginous layer's being a sub-aerial exposure surface: its regional extent, and mineralogical and sedimentological characteristics (Bhatt et al. 1981; Bhargava 1987; Singh et al. 1995; Srikantia and Bhargava 1998; Algeo et al. 2007; Williams et al. 2012). However, Himalayan Tethyan stratigraphy reflects a major sporadic transgression which commenced in the Mid-Early Permian and proceeded through the remainder of the Permian (Gardner 1992; Garzanti et al. 1996).

3 Sampling and analytical methods

Stratigraphically well-known Permo-Triassic sections exposed at Guryul Ravine ((Fig. 2a, b) and Attargoo village (Fig. 2c, d) of the Spiti region, Himachal Pradesh, northern India, were sampled for major elemental analysis. Weathered surfaces were trenched about 10–15 cm into the rock face and about 5-10 cm-

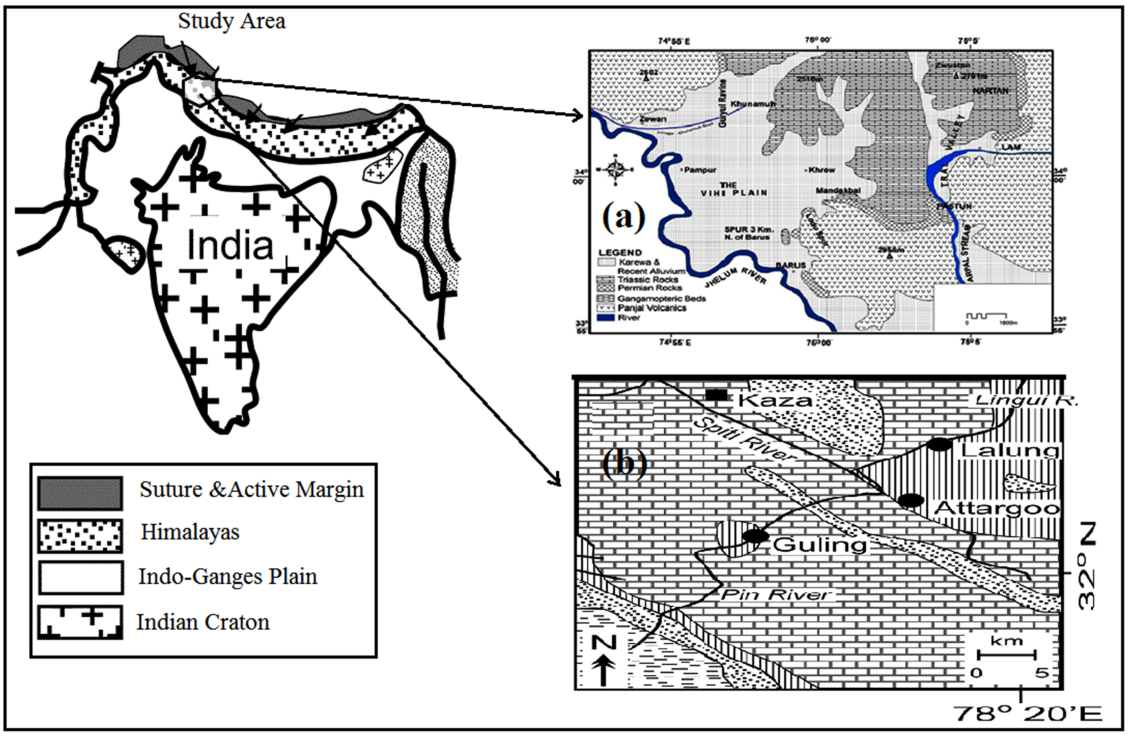

Fig. 1 **a** General geological map of Guryul Ravine section, Kashmir Region Jammu and Kashmir, India (after Bhat and Bhat 1997). **b** General geological map of Attargoo section, Spiti Region, Himachal Pradesh, India (after Shukla et al. 2002)

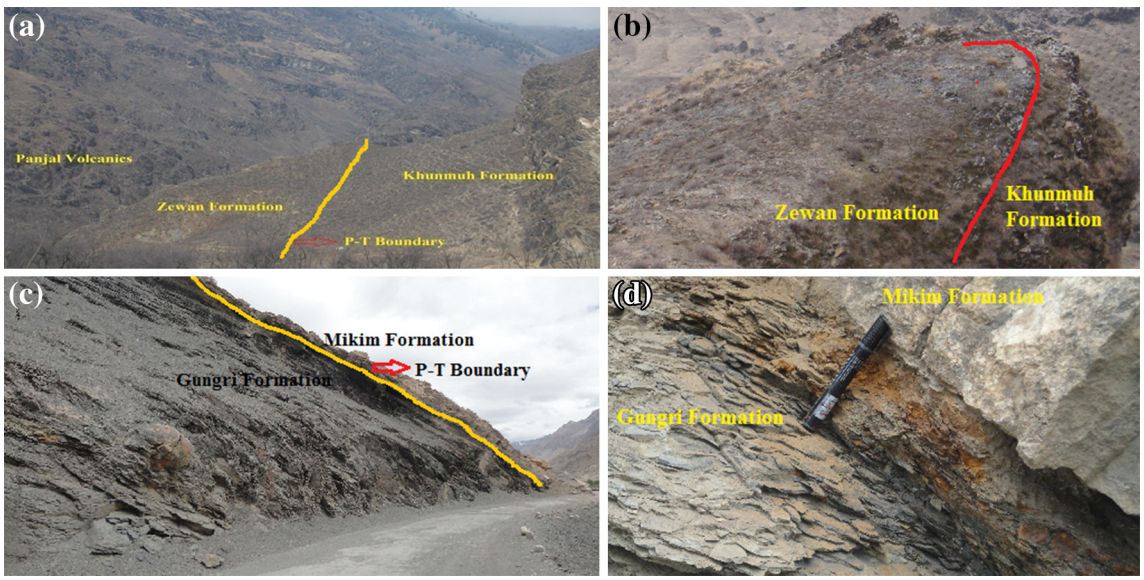

Fig. 2 **a** and **b** Field photograph showing close view of the Permian–Triassic boundary at Guryul Ravine section, Kashmir region Jammu and Kashmir, India; **c** and **d** Field photograph showing Permian–Triassic boundary at Attargoo section, Spiti Region, Himachal Pradesh, India

thick fresh chips from different rock types such as sandstones and shales were taken as samples. The fresh samples were put into polythene bags and placed into sealed bags marked with sample number and location, and transported to the Laboratory for chemical analysis. Geochemical analysis was carried out at the National Geophysical Research Institute (NGRI), Hyderabad, India. Samples were crushed and then powdered to 200 mesh size in an agate mill. Major elements were determined

from pressed pellets, which were prepared by using collapsible aluminum cups. These cups were filled with boric acid. About 1 g of powdered rock sample was put on top of the boric acid and the cups were then pressed under a hydraulic press at 20 tons pressure. The sample pellets were analyzed using a Philips MagiX PRO model PW-2440 wavelength dispersive X-ray fluorescence spectrometer (XRF) coupled with automatic sample changer PW 2540. International rock standards GSR-4 and GSR-5 were used as reference material during major element analysis. The precision and accuracy of the data are well within the international standards and are better than 5 %.

4 Geochemistry

The major elemental concentrations of both the Guryul Ravine and Attargoo Permian–Triassic sections are presented in Table 1. SiO_2 and Al_2O_3 concentrations of sandstones from the Guryul Ravine section ranged from 75 to 81 and 3.8 to 5.5 wt.%, respectively. MgO and Fe_2O_3 contents of sandstones from the Guryul Ravine section varied from 3.9 to 4.07 and 6.9 to 7.2 wt.%, respectively. Alkalis and alkaline earth elements (Na_2O, K_2O, CaO) are more depleted than other major elements in the sandstone of the Guryul Ravine section. The shales of the Guryul Ravine and Attargoo sections showed SiO_2 concentration between 55 and 77 and 49 and 65 wt.%, respectively. The lower SiO_2 content observed in some samples suggests possible hydraulic sorting during sedimentary processes. Al_2O_3 concentration of shales from the Guryul Ravine and Attargoo sections, varied from 11 to 17 and 16 to 20 wt.%, respectively, whereas TiO_2 ranges of the two sections were from 1.5 to 2.2 and 0.7 to 2 wt.%, respectively, and $Fe_2O_3^t$ contents varied from 0.79 to 10 and 2.9 to 17 wt.% respectively. Collectively, these results reveal the presence of a mixed clay assemblage and detrital phases in the shales.

When compared to Post-Archean Australian Shale (PAAS, after Taylor and McLennan 1985) values of shale samples of both sections are characterized by enrichment of TiO_2, MgO, and K_2O. Elevated K_2O (Fig. 3) concentration is attributed to contribution of K-feldspars and weathering of plagioclase feldspars. Enrichment of MgO with respect to PAAS may be attributed to the contribution of these elements from the marine fauna. SiO_2 and Al_2O_3 are more or less similar to PAAS in the shales of both sections. Further, shale samples showed depletion of Fe_2O_3 and P_2O_5; however, depletion of these oxides was greater in the case of the Guryul Ravine shales. Depletion of Fe_2O_3 and P_2O_5 in shales indicates the presence of relatively lesser quantities of phyllosilicates, ferromagnesian and apatite minerals, and/or may be attributed to the influence of degree of chemical weathering of the source rocks.

According to Cox et al. (1995), the K_2O/Al_2O_3 ratio relates to how much alkali feldspar versus plagioclase and clay minerals may have been present in the original shales. In order from high to low values, the K_2O/Al_2O_3 ratio of minerals represents alkali feldspars (0.4–1), illite (0.3), and other clay minerals (nearly 0). Shales with K_2O/Al_2O_3 greater than 0.5 are likely to possess a significant quantity of alkali feldspar relative to other minerals in the original shale, whereas those with K_2O/Al_2O_3 less than 0.4 likely possess minimal alkali feldspar in the original shale (Cox et al. 1995). The studied shales of the Guryul Ravine sections have average $K_2O/Al_2O_3 = 0.23$ (range 0.11–0.35); shales of the Attargoo section have average $K_2O/Al_2O_3 = 0.26$ (range 0.25–0.29). These overall low K_2O/Al_2O_3 ratios in the studied shales suggest minimal involvement of alkali feldspar relative to other minerals and strongly support that K_2O addition to the present samples has not taken place.

The enrichment of essential rock-forming minerals (if any) and altered products was determined by using the index of compositional variability (ICV). This parameter is calculated as $ICV = (Fe_2O_3 + K_2O + Na_2O + CaO + MgO + MnO + TiO_2)/Al_2O_3$ (Cox et al. 1995). Rock-forming minerals such as plagioclase, K-feldspars, amphiboles, and pyroxenes show ICV values of >0.84, whereas typical alteration products such as kaolinite, illite, and muscovite show values of <0.84 (Cox et al. 1995; Cullers 2000). The ICV values of sandstones and shales of the Guryul Ravine section range from 0.68 to 3.35 with an average of 1.69; shales of the Attargoo section show ICV from 0.68 to 1.62 with an average of 1.06. Hence, in both sections ICV values are greater than 0.84, indicating that the studied samples are enriched in rock-forming minerals. Quartz is more resistant to weathering than feldspars, mafic minerals, and lithics (Roser and Korsch 1986, 1999). Hence, SiO_2/Al_2O_3 ratio of siliciclastic rocks can be used to indicate sediment maturity. The average values of SiO_2/Al_2O_3 ratio in fresh igneous rocks ranges from $\sim$3.0 (in basic rocks) to $\sim$5.0 (in acidic rocks). The high SiO_2/Al_2O_3 values found in our analysis (Table 1) indicate relatively high sediment maturity (Roser and Korsch 1999).

5 Discussion

5.1 Paleo-weathering

Chemical weathering strongly affects major element geochemistry of siliciclastic sediments, as labile cations (e.g., Ca^{2+}, Na^+, K^+) are removed preferentially over more stable components (Al, Ti) (Nesbitt and Young 1982; Fedo et al. 1995). The degree of this weathering of feldspars is often measured relative to unweathered protoliths using the

Table 1 Major element concentrations of sandstones and shales from the Permain-Traissic sections at Kashmir and Spiti regions, Tethys Himalaya

Formation	Zewan Fm.				Khunamuh Fm.				Gungri Fm.								
Rock type	Sandstones				Shales				Shales								
Sample no.	Z-3	Z-4	Z-5	Z-6	K-1	K-2	K-3	K-4	G-1	G-2	G-3	G-4	G-5	G-6	G-7	G-8	G-9
SiO_2	81.34	75.89	78.65	55.74	77.88	65.25	66.24	68.30	58.58	49.40	59.99	65.06	60.09	52.89	60.43	60.79	56.07
TiO_2	0.69	0.77	0.67	1.93	1.53	2.15	1.75	2.23	2.13	0.77	1.01	1.05	1.01	0.87	1.01	0.97	0.92
Al_2O_3	4.32	5.50	3.89	17.51	11.23	16.99	14.66	15.67	19.43	15.15	19.88	20.30	19.13	16.53	20.46	19.41	18.82
Fe_2O_3	7.17	6.17	6.89	10.42	0.79	2.19	1.13	6.30	8.29	17.01	5.19	2.97	6.21	11.92	4.17	5.51	6.96
MnO	0.01	0.02	0.10	0.02	0.00	0.00	0.00	0.01	7.14	1.31	7.81	7.33	5.21	2.57	1.38	2.75	3.99
MgO	4.03	4.07	3.98	6.41	0.70	1.46	1.75	5.23	0.65	0.30	0.58	0.89	0.51	0.27	1.40	1.01	0.97
CaO	0.79	0.89	0.67	2.04	0.10	0.31	0.73	0.93	0.37	0.43	0.21	0.21	0.24	0.25	0.22	0.23	0.22
Na_2O	0.13	0.16	0.21	0.47	0.67	0.63	0.65	0.37	0.43	0.40	0.49	0.62	0.46	0.53	0.62	0.71	0.66
K_2O	0.46	0.62	0.53	4.68	3.92	5.58	4.76	3.75	5.32	4.34	5.47	5.40	5.47	4.54	5.16	4.88	4.85
P_2O_5	0.22	0.24	0.21	0.12	0.07	0.04	0.05	0.06	0.12	0.11	0.12	0.12	0.12	0.11	0.11	0.12	0.11
Sum	99.16	94.33	95.80	99.34	96.89	94.60	91.72	102.8	111.76	98.10	108.41	110.13	105.31	98.85	102.39	103.03	101.10
LOI	1.85	2.54	2.30	5.19	3.04	4.14	5.32	1.23	9.31	8.89	7.66	6.19	6.87	8.37	7.44	6.65	7.53
Al_2O_3/TiO_2	6.26	7.14	5.81	9.07	7.34	7.90	8.38	7.03	9.12	19.59	19.69	19.27	18.94	19.07	20.25	20.01	20.53
K_2O/Na_2O	3.54	3.88	2.52	9.96	5.85	8.86	7.32	10.14	12.38	10.84	11.16	8.71	11.98	8.51	8.33	6.88	7.38
CIA	67	68	65	73	67	69	66	71	73	71	74	74	73	73	74	74	74
CIW	72	75	71	80	90	91	86	87	93	91	94	94	94	93	94	92	93
PIA	70	72	68	74	84	87	80	83	91	88	92	91	92	90	91	90	90

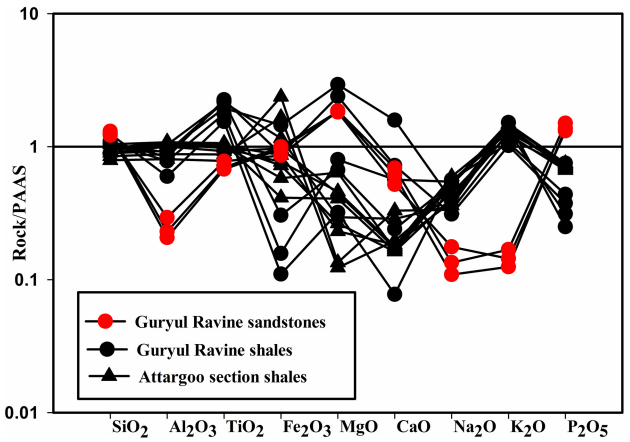

Fig. 3 Post-Archean Australian average Shale normalized major element patterns of the siliciclastic sediments (PAAS values after Taylor and McLennan 1985)

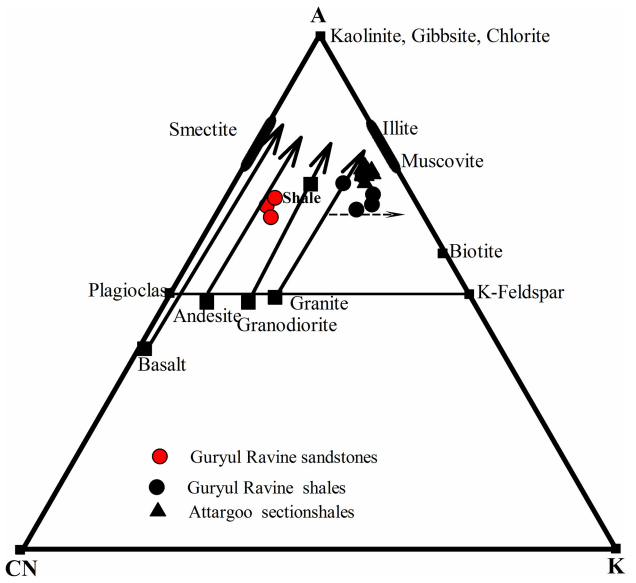

Fig. 4 A-CN-K ternary diagram (after Nesbitt and Young 1982) of sandstone and shales from the Permo-Triassic sections of Kashmir and Spiti regions Tethys Himalaya showing weathering trends. $A = Al_2O_3$; $CN = (CaO^* + Na_2O)$; $K = K_2O$ (all in molar proportions)

chemical index of alteration (CIA)(Nesbitt and Young 1984). CIA is defined by the equation: $CIA = [Al_2O_3/(Al_2O_3 + CaO^* + Na_2O + K_2O] \times 100$ where all elements are in molecular proportion, and CaO* represents Ca in the silicate fraction only. As the sample Z6 contains CaO greater than 1 wt.%, there would be a chance of presence of organic content or presence of Ca in carbonates (calcite, dolomite). It is therefore necessary to correct for the measured CaO content in the samples. Due to non-availability of a direct method to distinguish and quantify the amount of CaO belonging to the silicate and non-silicate fractions, a method proposed by McLennan (1993) has been used to calculate the CaO* in the present study. According to this method, if the number of moles of CaO is less than that of Na_2O, then the pure CaO value can be adopted. If the number of moles for CaO is greater than Na_2O, CaO* should be assumed to be equivalent to Na_2O. CIA values for average shales range from 70 to 75 which reflect a composition of muscovite, illite, and smectite. Intensely weathered rock yields mineral compositions trending toward kaolinite or gibbsite and a CIA approaching 100. CIA of unweathered rock is about 50. The studied sandstone and shales of the Guryul Ravine section have CIA values from 65 to 73; Attargoo section shales have CIA values from 71 to 74, reflecting their composition of muscovite and illite. The weathering trend can be illustrated on the triangular Al_2O_3, $CaO^* + Na_2O$, K_2O (A–CN–K) plot, which is useful for evaluating and correcting the effects of K-metasomatism and giving some information of the composition of the fresh source rock (Fedo et al. 1995). On this diagram (Fig. 4), studied samples plot towards the A–K line away from the plagioclase-K-feldspar join, indicating low to moderate degree of weathering. Chemical weathering can also be measured by chemical index of weathering (CIW, Harnois 1988) and plagioclase index of alteration (PIA, Fedo et al. 1995). CIW eliminates the effect of K-metasomatism and is calculated as: $CIW = Al_2O_3/(Al_2O_3 + CaO^* + Na_2O) \times 100$ where the elements are represented in mole proportion and CaO* represents Ca in the silicate fraction. Most strikingly, unweathered potassic granite has a CIW of 80 and fresh K-feldspar has a CIW of 100, similar to values for residual products of chemical weathering (smectite CIW = 80; kaolinite, illite, and gibbsite CIW = 100).The CIW values of Guryul Ravine sandstone and shales range from 71 to 91; the CIW of Attargoo section shales from 91 to 94. This indicates a much reduced K-metasomatism effect on the samples of the study area. PIA reflects weathering of plagioclase feldspars and is defined by the equation: $PIA = [(Al_2O_3–K_2O)/(Al_2O_3 + CaO^* + Na_2O–K_2O)] \times 100$, where all elements are in molecular proportions and CaO* represents CaO in silicate fractions. The maximum PIA value is 100 (kaolinite, gibbsite) and unweathered plagioclase has PIA value of 50. Studied sandstone and shale samples of Guryul Ravine section have PIA values from 68 to 87. However, shale of the Attargoo section has slightly higher PIA values of 88 to 92. Therefore, PIA values in studied samples indicate a moderate degree of weathering of plagioclase feldspars in both the Permo-Triassic sections.

5.2 Provenance and tectonic setting

Geochemical composition of basin sediments is changed to some extend by various processes such as hydraulic

sorting, weathering, and diagenesis. However, strong signatures of the original source terrain are stored in these sediments, thus reflecting the nature of the exposed continental crust. Because of low solubility of Al and Ti oxides and hydroxides at low temperatures, these elements are generally stable in the face of siliciclastic weathering (Sugitani et al. 2006). For this reason, Al/Ti ratios of residual soils is believed to be very close to those of their parent material allowing this ratio to be used by various researchers for discrimination of provenance (e.g., Hayashi et al. 1997; Sugitani et al. 2006; Odigi and Amajor 2008; Sun et al. 2013; Ganai et al. 2014; Mir et al. 2015). Studies have shown that Al_2O/TiO_2 ratios ranging from 3 to 8 indicate mafic igneous rocks, from 8 to 21 intermediate rocks, and from 21 to 70 felsic igneous rocks. In our samples Al_2O/TiO_2 ratio varied from 6 to 20, which indicates an intermediate source (Hayashi et al. 1997; Sugitani et al. 2006). McLennan et al. (1980), recognizing the significance of Al and Ti in provenance studies, proposed an Al_2O_3 versus TiO_2 bivariate discrimination diagram to constrain the provenance of siliciclastic rocks. On this diagram, the siliciclastic sediments of the study areas plot along granitic and 3 granite +1 basalt trend lines indicating felsic provenance (Fig. 5). The major element–based provenance discriminant function diagram of Roser and Korsch (1988) is frequently used by many researchers to identify the provenance of terrigenous sediments (Cullers 2000; Islam et al. 2002; Rashid 2005; Dey et al. 2009). This diagram discriminates four major provenance fields: mafic, intermediate, felsic, and quartzose sedimentary. Studied Guryul Ravine section samples fall within the Quartzose sedimentary provenance and those of the Attargoo section fall into the Felsic igneous provenance (Fig. 6). However, for further verification of provenances of the studied samples from both PTB sections, it is recommended to use trace element or isotope data.

Several studies have revealed that the chemical compositions of siliciclastic rocks are significantly controlled by plate tectonic settings of their provenances, and consequently siliciclastic rocks from different tectonic settings possess terrain-specific geochemical signatures (Bhatia and Crook 1986; Roser and Korsch 1986; Li et al. 2003). Tectonic settings of provenances of ancient siliciclastic rocks can be inferred from the major element–based discrimination diagrams proposed by Roser and Korsch (1986) by utilizing (K_2O/Na_2O) versus SiO_2. Both SiO_2 and K_2O/Na_2O values increase from volcanic arc to active continental margin to passive margin settings; high SiO_2 and low Na_2O in the binary discriminant plots suggest

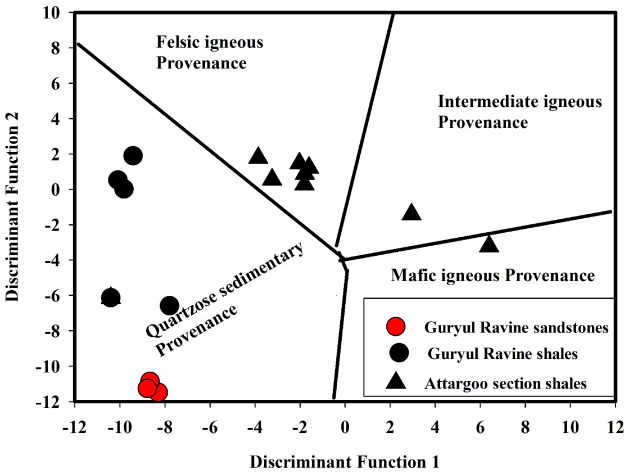

Fig. 6 Major element provenance discriminant function diagram (after Roser and Korsch 1988) for siliciclastic sediments of Permo-Triassic sections of Kashmir and Spiti regions Tethys Himalaya

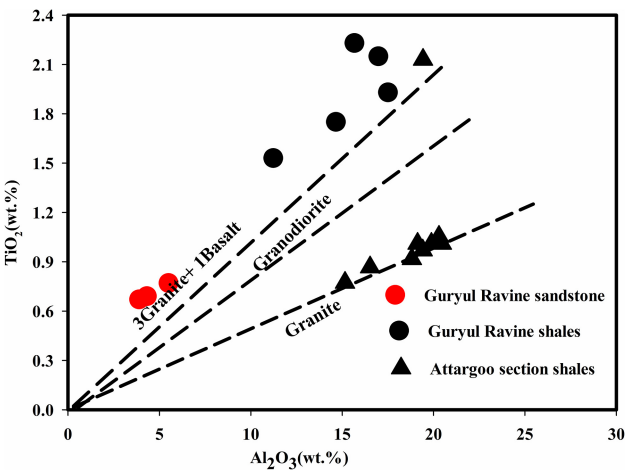

Fig. 5 Al_2O_3 versus TiO_2 bivariate diagram (after McLennan et al. 1980)

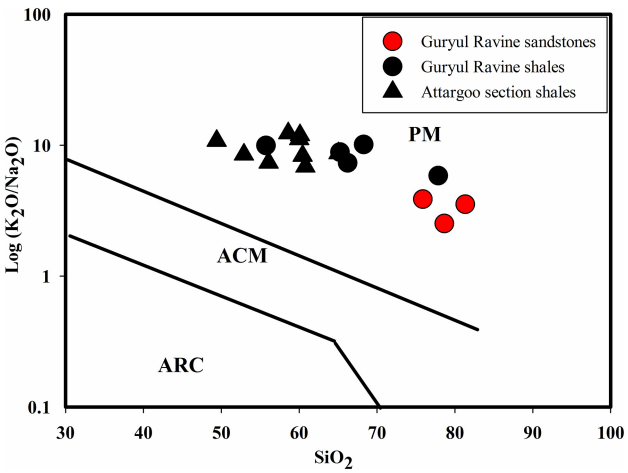

Fig. 7 K_2O/Na_2O versus SiO_2 discrimination diagram (after Roser and Korsch 1986) for siliciclastic sediments of Permo-Triassic sections of Kashmir and Spiti regions Tethys Himalaya

continentally-derived sediments. In the SiO_2 versus K_2O/Na_2O diagram, samples from both Permo-Triassic sections (Guryul Ravine and Attargoo) in this study plot in the field of passive continental margin setting (Fig. 7).

6 Conclusions

As expected, geochemically the sandstones of the Permian–Triassic sections of the NW Tethys Himalaya, India are more enriched in SiO_2 and show significant variations in other major elemental abundances. When compared to UCC, the alkalis and alkaline earth elements (Na_2O, K_2O, MgO, and CaO) are more depleted than other elements in the samples. The salient geochemical characteristics (such as enrichment in felsic elements and their ratios with depleted mafic components) indicate the Permo-Triassic siliciclastic sedimentary rocks of the Guryul Ravine and Attargoo sections may be derived from a felsic-dominant source i.e. quartzose sedimentary and granitic rocks and may have been deposited in a passive continental margin tectonic setting. On the bases of CIA and CIW it is concluded that studied samples of the Permo-Triassic sections experienced low to moderate degree of chemical weathering. PIA values in studied samples show moderate weathering of plagioclase feldspars. The consistent variation in terms of degree of chemical weathering noticed in the sandstones and shales from the studied PTB sections clearly indicates climatic influence in the deposition of the Tethys sediments.

Acknowledgments We are thankful to the Director, NGRI, Hyderabad for permission to analyze the studied samples. First and third authors pay sincere gratitude to Prof. Shakil A. Romshoo, Head, Department of Earth Sciences, University of Kashmir for providing necessary facilities. Authors pay our sincere thanks to reviewers for their constructive comments and suggestions.

References

Algeo TJ, Hannigan R, Rowe H, Brookfield M, Baud A, Krystyn L, Ellwood BB (2007) Sequencing events across the Permian–Triassic boundary, Guryul Ravine (Kashmir India). Palaeogeogr Palaeoclimatol Palaeoecol 252:328–346

Benton MJ, Tverdokhlebov VP, Surkov MV (2004) Ecosystem remodelling among vertebrates at the Permian–Triassic boundary in Russian. Nature 432:97–100

Berner RA (2002) Examination of hypotheses for the Permo-Triassic boundary extinction by carbon cycle modeling. Proc Natl Acad Sci USA 99:4172–4177

Bhargava ON (1987) Stratigraphy, microfacies and paleoenvironment of the Lilang Group (Scythian-Dogger), Spiti Valley, Himachal Himalaya, India. J Palaeontol Soc India 25:91–107

Bhargava ON (2008) An updated introduction to the Spiti geology. J Palaeontol Soc India 53:113–129

Bhat GM, Bhat GD (1997) Stratigraphy and depositional environment of Late Permian Carbonates, Kashmir Himalaya. Geol Surv Mines Bur Srilanka Prof Paper 7:205–223

Bhatia MR, Crook KAW (1986) Trace element characteristics of graywackes and tectonic setting discrimination of sedimentary basins. Contrib Miner Petrol 92:181–193

Bhatt DK, Fuchs G, Prashara KC, Krysten L, Arora RK, Golebiowski R (1981) Conodonts of otoceras beds of Spiti. J Palaeontol Soc India 25:130–134

Brookfield ME, Twitchett RJ, Goodings C (2003) Palaeoenvironments of the Permian-Triassic transition sections in Kashmir, India. Palaeogeogr Palaeoclimatol Palaeoecol 198:353–371

Brookfield ME, Shellnutt JG, Liang Qi R, Hannigan GM, Bhat PB Wignall (2010) Platinum element group variations at the Permo-Triassic boundary in Kashmir and British Columbia and their significance. Chem Geol 272:12–19

Brookfield ME, Algeo TJ, Hannigan R, Williams J, Bhat GM (2013) Shaken and stirred: seismites and tsunamites at the Permian–Triassic boundary, Guryul Ravine, Kashmir, India. Palaios 28:568–582

Cox R, Lowe DR, Cullers RL (1995) The influence of sediment recycling and basement composition on evolution of mudrock chemistry in the southwestern United States. Geochim Cosmochim Acta 59(14):2919–2940

Cullers RL (2000) The geochemistry of shales, siltstones and sandstones of Pennsylvanian-Permian age, Colorado, U.S.A: implications for provenance and metamorphic studies. Lithos 51:305–327

Dey S, Rai AK, Chaki A (2009) Palaeo-weathering, composition and tectonics of provenance of the Proterozoic Kaladgi Badami basin Karnataka southern India: evidence from sandstone petrography and geochemistry. J South Asian Earth Sci 34:703–715

Erwin DH (2005) Extinction: how life on earth nearly died 250 million years ago. Princeton University Press, Princeton

Fedo CM, Nesbitt HW, Young GM (1995) Unraveling the effects of potassium metasomatism in sedimentary rocks and paleosols, with implications for paleo-weathering conditions and provenance. Geology 23:921–924

Ganai JA, Shaik RA, Alam MM, Balaram V, Sathyanarayanan M (2014) The geochemistry of Permo-Carboniferous black shales from Spiti region, Himachal Pradesh, Tethys Himalaya: a record of Provenance and change in climate. Himal Geol 35(1):31–39

Gardner LR (1992) Long-term isovolumetric leaching of aluminum from rocks during weathering: implications for the genesis of saprolite. Catena 19:521–537

Garzanti E, Angiolini L, Sciunnach D (1996) The mid-carboniferous to Lowermost Permian succession of Spiti po group and ganmachidam formation Tethys Himalaya, northern India: gondwana glaciation and rifting of neo-tethys. Geodin Acta 9:78–100

Garzanti E, Angiolini L, Brunton H, Sciunnach D, Balini M (1998) The bashkirian fenestella shales and the moscovian chaetetid shales of the Tethys Himalaya: south Tibet, Nepal and India. J Asian Earth Sci 16:119–141

Harnois L (1988) The CIW index: a news index of weathering. Sed Geol 55:319–322

Hayashi K, Fujisawa H, Holland H, Ohmoto H (1997) Geochemistry of ~1.9 Ga sedimentary rocks from northeastern Labrador, Canada. Geochim Cosmochim Acta 61(19):4115–4137

Hongfu Y, Kexin Z, Jinnan T,Zunyi Y, Sunbao W (2001) The global stratotype section and point (GSSP) of the Permian–Triassic boundary. Episodes 24:102–114

Huey RB, Ward PD (2005) Hypoxia, global warming, and terrestrial Late Permian extinctions. Science 308:398–401

Islam R, Ghosh SK, Sachan HK (2002) Geochemical characterization of the Neoproterozoic Nagthat siliciclastics, NW Kumaun Lesser Himalaya: implications for source rock assessment. J Geol Soc India 60:91–105

Kapoor HM (1992) Permo-Triassic of the Indian subcontinent and its intercontinental correlation. In: Sweet WC, Yang Z, Dickins JM,

Yin H (eds) Permo-triassic events in the eastern tethys. Cambridge University Press, Cambridge, pp 21–36

Kapoor HM (1996) The Guryul ravine section, candidate of the global stratotype and point (GSSP) of the Permia-Triassic boundary (PTB). In: Yin H (ed) The paleozoic-mesozoic boundary. Candidates of the global stratotype section and point of the Permian–Triassic boundary. China University of Geosciences Press, Wuhan, pp 99–110

Maruoka T, Koeberl C, Hancox PJ, Reimold WU (2003) Sulfur geochemistry across a terrestrial Permian–Triassic boundary section in the Karoo Basin, South Africa. Earth Planet Sci Lett 206(1–2):101–117

McLennan SM (1993) Weathering and global denudation. J Geol 101:295–303

McLennan SM, Nance WB, Taylor SR (1980) Rare earth element-thorium correlation in sedimentary rocks and the composition of the continental crust. Geochim Cosmochim Acta 44:1833–1839

Mir AR, Bhat ZA, Alvi SH, Balaram V (2015) Geochemistry of black shales from Singhbhum mobile belt, Eastern India: implications for paleo-weathering and provenance. Himal Geol 36(2):126–133

Myrow PM, Hughes NC, Paulsen T, Williams I, Parcha SK, Thompson KR, Bowring SA, Peng SC, Ahluwalia AD (2003) Integrated tectonostratigraphic analysis of the Himalaya and implications for its tectonic reconstruction. Earth Planet Sci Lett 212:433–444

Nakazawa K, Kapoor HM (1981) The Upper Permian and Lower Triassic Faunas of Kashmir. Palaeontol Indica New Ser 46:1–191

Nakazawa K, Kapoor HM, Ishii K, Bando Y, Okimura Y, Tokuoka T (1975) The Upper Permian and the Lower Triasssic in Kashmir, India. Memoir Facul Sci Kyoto Univ Geol Mineral Ser 41:1–106

Nesbitt HW, Young GM (1982) Early Proterozoic climates and plate motion inferred from major element chemistry of lutites. Nature 299:715–717

Nesbitt HW, Young GM (1984) Prediction of some weathering trend of plutonic and volcanic rocks based on thermodynamic and kinetic consideration. Geochim Cosmochim Acta 48:1523–1534

Odigi MI, Amajor LC (2008) Petrology and geochemistry of sandstones in the southern Benue Trough of Nigeria: implications for provenance and tectonic setting. Chin J Geochem 27:384–394

Payne JL, Lehrmann DJ, Wei J, Orchard MJ, Schrag DP, Knoll AH (2004) Large perturbations of the carbon cycle during recovery from the End-Permian extinction. Science 305:506–509

Rashid SA (2005) The geochemistry of Mesoproterozoic clastic sedimentary rocks from the Rautgara Formation, Kumaun Lesser Himalaya: implications for provenance, mineralogical control and weathering. Curr Sci 88:1832–1836

Roser BP, Korsch RJ (1986) Determination of tectonic setting of sandstone-mudstone suites using SiO_2 content and K_2 O/Na_2O ratio. J Geol 94:635–650

Roser BP, Korsch RJ (1988) Provenance signatures of sandstone-mudstone suites determined using discriminant function analysis of major element data. Chem Geol 67:119–139

Roser BP, Korsch RJ (1999) Geochemical characterization, evolution and source of a Mesozoic accretionary wedge: the Torlesse terrane, New Zealand. Geol Mag 136:493–512

Saito Y (1989) Modern storm deposits in the inner shelf and their recirrence intervals, Sendai Bay, northeast Japan. In: Taira A, Masuda F (eds) sedimentary facies in the active plate margin. Terra Science Publishing, Tokyo, pp 331–344

Sciunnach D, Garzanti E (2012) Subsidence history of the Tethys Himalaya. Earth Sci Rev 111:179–198

Shen W, Lin Y (2010) Environmental conditions and events prior to the Permian–Triassic boundary at Meishan Section, China. J Earth Sci 21:151–153

Shen W, Sun Y, Lin Y, Liu D, Chai P (2011) Evidence for wildfire in the Meishan section and implications for Permian–Triassic events. Geochim Cosmochim Acta 75:1992–2006

Shukla AD, Bhandari N, Shukla PN (2002) Chemical signatures of the Permian–Triassic transitional environment in Spiti Valley, India. In: Koeberl C, MacLeod KG (eds) Catastrophic events and mass extinctions: impacts and beyond. Geological Society of America, Boulder, pp 445–453

Sing, J, Mahanti S, Singh K (2004) Geology and evaluation of hydrocarbon prospects of Tethyan sediments in Spiti Valley, Spiti and Zanskar, Himanchal Pradesh, 19th Himalaya-Karakoram-Tibet Workshop. Himalayan Journal of Sciences, Niseko pp 250

Singh T, Tiwari R, Vijaya S, Avtar R (1995) Stratigraphy and palynology of Carboniferous-Permian–Triassic succession in Spiti Valley, Tethys Himalaya, India. J Palaeontol Soc lndia 40:55–76

Srikantia SV, Bhargava ON (1998) Geology of Himachal Pradesh: Geological Society of India, Bangalore p 416

Sugitani K, Fumiaki Y, Tsutomu N, Koshi Y, Masayo M, Koichi M, Kazuhiro S (2006) Geochemistry and sedimentary petrology of Archean clastic sedimentary rocks at Mt. Goldsworthy, Pilbara Craton, Western Australia: evidence for the early evolution of continental crust and hydrothermal alteration. Precambr Res 147:124–147

Sun L, Gui H, Chen S, Ma Y, He Z (2011) Geochemical characteristics and geological significance of the Neoproterozoic carbonates from northern Anhui Province, China. Chin J Geochem 30:40–50

Sun L, Gui H, Chen S (2013) Geochemistry of sandstones from the Neoproterozoic Jinshanzhai Formation in northern Anhui Province, China: provenance, weathering and tectonic setting. Chin J Geochem 32:095–103

Taylor SR, McLennan SM (1985) The continental crust: its composition and its evolution. Blackwell, Oxford

Wani H, Mondal MEA (2011) Evaluation of provenance, tectonic setting, and paleoredox conditions of the Mesoproterozoic-Neoproterozoic basins of the Bastar craton, Central Indian Shield: using petrography of sandstones and geochemistry of shales. Lithosphere 3:43–154

Wignall PB, Twitchett RJ (1996) Oceanic anoxia and the Permian mass extinction. Science 272:1155–1158

Williams JC, Basu AR, Bargava ON, Ahluwalia AD, Hannigan RE (2012) Resolving original signatures from a sea of overprint- The geochemistry of the Gungri Shale (Upper Permian) Spiti Valley India. Chem Geol 324:59–72

Xu L, Lin Y (2014) Analysis of platinum-group elements in drill core samples from the Meishan Permian–Triassic boundary section, China. Chin J Geochem 33:365–373

Zhang Z, Yang X, Li S, Zhang Z (2010) Geochemical characteristics of the Xuanwei Formation in West Guizhou: significance of sedimentary environment and mineralization. Chin J Geochem 29:355–364

Zhiming L, Jiajun L, Ruizhong H, Mingqin H, Yuping L, Chaoyang L (2003) Tectonic setting and nature of the provenance of sedimentary rocks in Lanping Mesozoic-Cenozoic Basin: evidence from geochemistry of sandstones. Chin J Geochem 22:352–360